



PERFORMANCE COMPARISON OF RC RETROFITTED INTERIOR BEAM-COLUMN JOINTS WITH CFRP AND STEEL PLATES

J. Melo⁽¹⁾, D. Pohoryles⁽²⁾, T. Rossetto⁽³⁾, H. Varum⁽⁴⁾

⁽¹⁾ Research Associate, EPICentre, University College London, U.K., jose.melo.11@ucl.ac.uk

⁽²⁾ PhD Candidate, EPICentre, University College London, U.K., daniel.pohoryles.10@ucl.ac.uk

⁽³⁾ Professor, EPICentre, University College London, U.K.

⁽⁴⁾ Professor, CONSTRUCT, Faculty of Engineering of the University of Porto, Portugal

Abstract

Existing reinforced concrete (RC) building structures constructed until the mid-1970's, prior to the enforcement of modern seismic design philosophies, are expected to behave poorly when subjected to earthquake actions. The response and damage evolution of RC structures when subjected to severe cyclic loading, such as the ones induced by earthquakes, are highly influenced by the beam-column joint behavior, as they are responsible for the force transfer mechanism between columns and beams and restrain the lateral displacement of the columns.

The seismic response of existing RC structures with inadequate reinforcement detailing in the beam-column connections can be improved by retrofitting these connections. In the literature several joint retrofit techniques are presented, including concrete or steel jacketing, carbon fiber reinforced polymer (CFRP) wrapping and strengthening with steel profiles, plates or angles. These retrofit techniques aim to avoid the weak-column/strong-beam mechanism by increasing the flexural capacity of the column and also, in some cases, to improve the joint shear capacity.

In this paper a series of unidirectional cyclic tests carried out on four full-scale interior beam-column joints with transverse beams and slab, with typical detailing of structures built until the mid-70's, are described. One specimen is tested without retrofit (control specimen), another is retrofitted with CFRP and the other two are retrofitted with steel profiles and plates. Both retrofit solutions aim to increase the flexural strength of the columns and the joint shear capacity and to avoid the weak-column/strong-beam mechanism identified in the control specimen test. The selective weakening technique is applied to all retrofitted specimens by cutting the slab in both directions around the joint. The main results in terms of lateral force-displacement, equivalent damping, ductility and dissipated energy evolution diagrams, as well as damage description at the end of the tests are presented and discussed. The experimental results show that the adopted retrofit solutions can significantly increase the maximum lateral strength, the ultimate ductility and the energy dissipation capacity. Therefore, the improved seismic performance of the retrofitted specimens is evident when compared with the control specimen and consequently demonstrates the need of retrofitting beam-column joints in order to improve the global seismic behavior of existing RC structures.

Keywords: RC retrofitting; Beam-column joint; Full-scale testing; existing RC structures



1. Introduction

The number of existing reinforced concrete (RC) structures built prior to the enforcement of modern seismic-design codes is significant. As a consequence, inadequate structural performance even under moderate seismic excitations is expected in the majority of these structures due to the lack of ductility at both the local and global levels. Beam-column joints have a large influence on the cyclic behaviour of RC structures and the premature failure of joints has to be prevented, as the failure of these elements usually leads to full collapse of the structure. The lack of seismic design for existing RC structures often causes weak-column/strong-beam mechanisms that induce premature failure of columns or beam-column joints as described in several field mission reports [1, 2].

The seismic performance of existing non-seismic RC structures can be improved by applying retrofit solutions that increase the ductility and/or strength of critical RC elements. Several traditional retrofit solutions for RC elements are available in the literature, including fibre reinforced polymers (FRP) wrapping and concrete or steel jacketing. However, a significant part of experimental studies carried out to develop and assess these traditional solutions on beam-column joints were applied to specimens without transverse beams and slab or specimens that are less than full-scale, which does not represent real in-situ conditions well. Consequently, there is a need to develop and test new realistic retrofit arrangements and configurations as presented in this paper.

Previous experiments [3], highlighted that a change in hierarchy of strength, to comply with capacity design principles, may be prevented by the significant influence of slabs in the behaviour of retrofitted RC joints. To reduce the slab stiffness and strength contributions, the selective weakening (SW) technique was implemented on corner beam-column joints [4] and interior beam-column joints [5] by cutting the slab reinforcement along the potential plastic hinge zone of the beam, without considerably changing the global strength of the slab.

In this paper, results from full-scale cyclic tests on new retrofit schemes for realistic interior RC beam-column joints are presented and compared with the results of a control specimen. The detailing adopted for the specimens represents the typical detailing of structures built until the mid-70's. A retrofit solution with CFRP and another one with steel plates combined with selective weakening of the slab are developed and implemented. Additionally, a cyclic test on a repair and retrofit specimen with steel plates is presented. The adopted retrofit solutions aim to increase the lateral capacity of the, enhance the ductility and change the failure mechanism to a ductile weak-beam/strong-column failure mechanism. The main results obtained in terms of strength, equivalent damping, ductility, dissipated energy evolution, and the damage at the end of the tests are presented and discussed.

2. Material properties, specimens details and test setup

2.1. Beam-column joint specimens detailing

Four full-scale RC interior beam-column joints with transverse beams and slab are built and tested under uniaxial cyclic lateral loading. These tests are part of a larger experimental campaign performed to assess and develop new retrofit solutions for realistic interior beam-column joints. The specimens presented here include one control (C-SW), one retrofit with CFRP (C1-RT-B SW), one repair (C1-RP-Steel SW) and one retrofit (C1-RT-Steel SW) specimen with steel plates. After the test of specimen C-SW, it is repaired and retrofitted with steel plates and tested again under the name of C1-RP-Steel SW.

The specimens are designed to represent real-scale interior beam-column joints in a four-storey RC frame structure. Each column represents a half-storey 1.50m column with a square cross-section of 300mm by 300mm. Similarly, each beam represents a 2.00m rectangular half-span beam with a cross-section of 450mm deep to 300mm wide. The slab has a depth of 150mm and is 1.95m wide.

The four specimens have the same reinforcement detailing and geometry and are representative of RC elements designed according to codes enforced in Southern Europe before the mid-1970's area. The limits given

in the REBA (1967) [6] Portuguese RC code are followed and a seismic factor for lateral load of 0.05 is chosen as suggested in the code. The reinforcement detailing and geometry adopted can be seen in Fig.1.

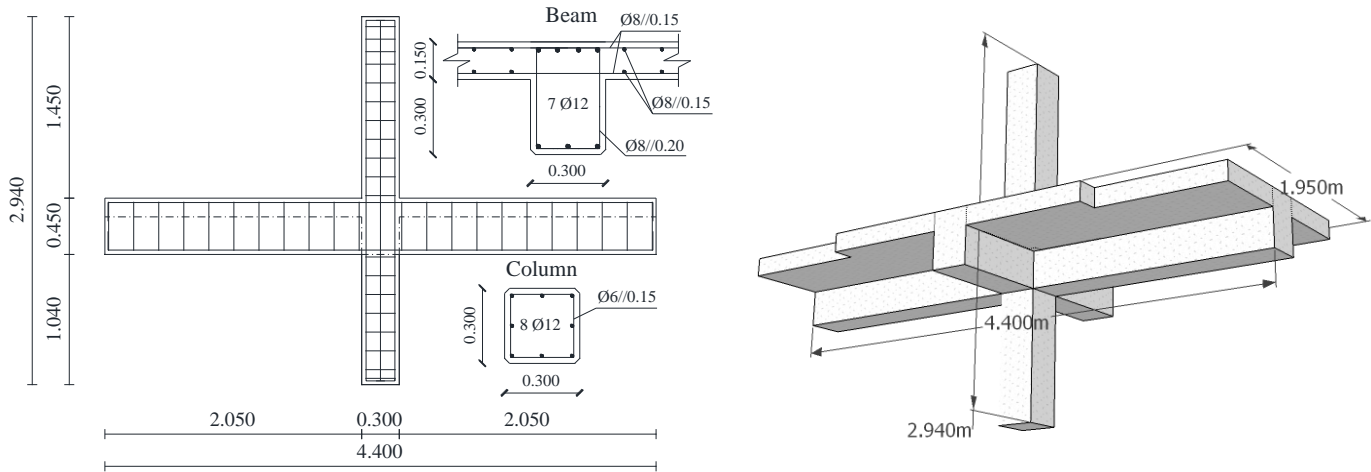


Fig. 1 – Geometry, dimensions and reinforcement detailing of the specimens (in m)

The design adopted leads to seismic deficiencies typically found from pre-1970's, designs, namely: lower flexural capacity of the columns than the beams; lower shear capacity of the joint due to the lack of transverse reinforcement in the core joint; and inadequate transverse reinforcement spacing in the columns and beams that provide a lack of confinement.

The flexural and shear capacities of the columns and beams are individually calculated according to Eurocode 2 [7], to assess the potential failure mechanisms and help on the design of the retrofit solutions adopted. It is found that the bending capacity of the columns is lower than the flexural capacity of the beams, therefore severe damage on the columns and minor damages on the beams is expected. Moreover, due to the contribution of the slab and the asymmetric reinforcement in the beams, the capacity of the beams for hogging moments is much larger than the capacity for sagging moments and the top of the beam is much stiffer than the bottom. Less rotation in the beams and consequently less damage are expected on the beams. The selective weakening technique initially developed by [8] is adopted to reduce the stiffness provided by the slab in all specimens here presented. The stiffness contribution of the slab is reduced by making cuts through the slab (including rebars) with 0.60m length from the column in both directions. The cuts are parallel to the longitudinal beam and transversal beam. Specimens without cuts on the slab were also tested, but the results are presented in another study [3].

Table 1 – Mean values of the material mechanical properties

Specimen	f_{cm} [MPa]	$f_y/f_u - \Phi 12$ [MPa]	$f_y/f_u - \Phi 8$ [MPa]	$f_y/f_u - \Phi 6$ [MPa]	$f_{u,FRP}$ [MPa]
C-SW	26.0	450/570	540/640	538/645	3300
C1-RP-Steel SW	26.5				
C1-RT-Steel SW	19.3				

The specimens are casted on different days using the same formwork, in a vertical position. Compressive tests of concrete cylinder samples (Ø150mmx300mm) were made for determining the concrete properties used in each specimen. Moreover, tensile strength tests on steel and FRP S&P C-240 sheet are performed to characterize the materials used in each specimen. For the FRP tensile strength, the method in ISO/DIS 10406-2:2013 was used. Table 1 summarizes the mean values of the material properties, where f_{cm} is the mean concrete

compressive strength of cylinder samples, f_{ym} is the yield strength of reinforcement steel, f_{um} is the ultimate tensile strength of reinforcement and $f_{u,FRP}$ the rupture strength of FRP. In the steel retrofitting solution was used S355 grade steel. The concrete used to repair the column of specimen C-SW had $f_{cm}=36.9\text{MPa}$.

2.2. Test setup and loading history

The loading set-up of the specimens is shown in Fig.2. The specimens are tested in the horizontal position and six high load carrying capacity and reduced friction rollers are placed below the specimen to carry the elements' self-weight. The tests are performed under displacement controlled conditions.

Lateral displacements (d_c) are imposed by a hydraulic servo-actuator at the top of the upper column at 1.5m from the center of the joint core. A constant axial load ($N1$) of 425 kN is applied to the top and bottom of the columns. An additional axial load ($N2$) of 25 kN is applied at the bottom to induce moments in the beams, simulating moments from gravity loading. The cyclic lateral displacement history adopted consisted in: three cycles applied for each of the following peak drift values (\pm %): 0.1, 0.2, 0.3 and then 0.5 to 6.0 with 0.5 increments. The same displacement history was used in all specimens.

The experiments are monitored using eight strain gauges on the reinforcement (four on the superior column, one on the inferior column, two on the bottom beam bars and one on the top beam bars), four strain gauges on the FRP strands, 16 LVDT's, 28 potentiometers, four draw-wire position transducers, four inductive linear position sensors and three pairs of cameras for stereoscopic 3D-digital-image correlation (DIC). The DIC analysis is performed using the DaVis 8.2.3 software.

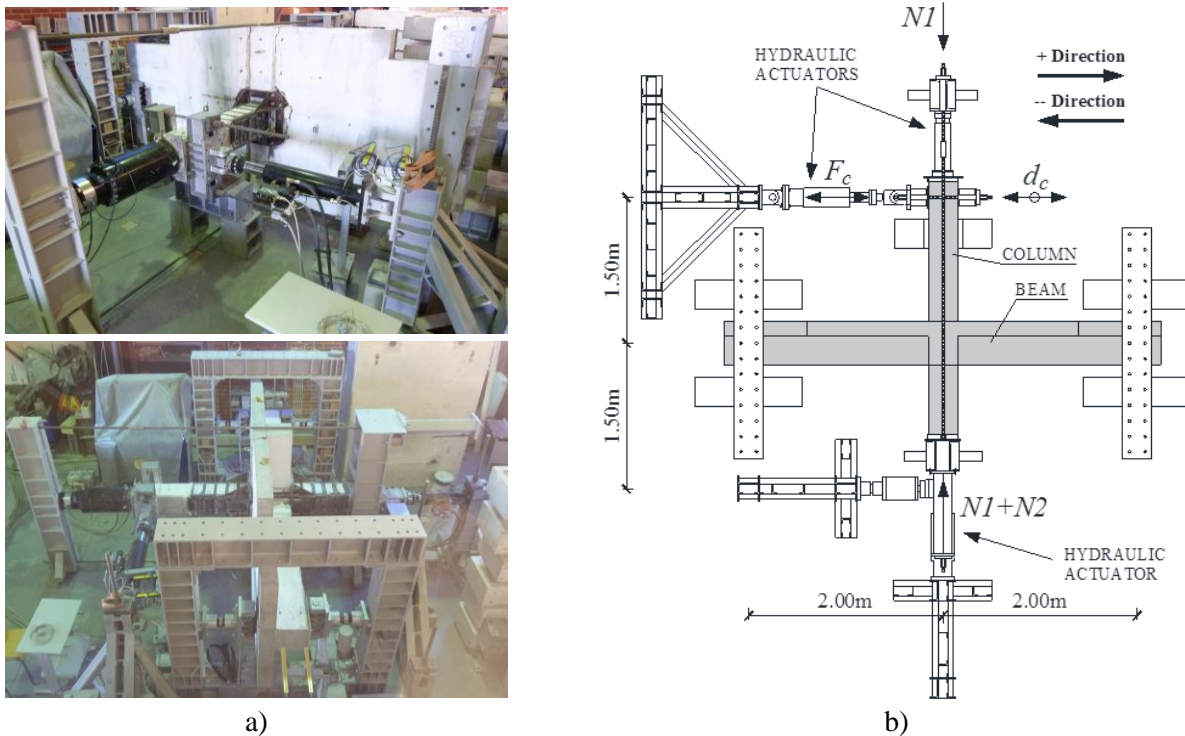


Fig. 2 – Interior beam-column joint test setup: a) general views; b) test setup schematics

3. CFRP and Steel plates retrofit schemes

3.1. CFRP retrofit scheme

The aim of the presented scheme is to offer a complete and realistic solution to increase flexural capacity of beams without increasing their stiffness, ensure plastic hinge forms in the beam, away from the joint, ensure flexural strength of column is higher than that of beams and strengthen the joint due to higher joint shear stresses. Moreover, the selective weakening technique used in the slab aims weaken the slab close to the core joint to ensure increased rotation of beams.

The details of the retrofit scheme developed and adopted on specimen C1-RT-B SW are shown in Fig.3. The full details regarding the CFRP retrofit scheme can be found on [9].

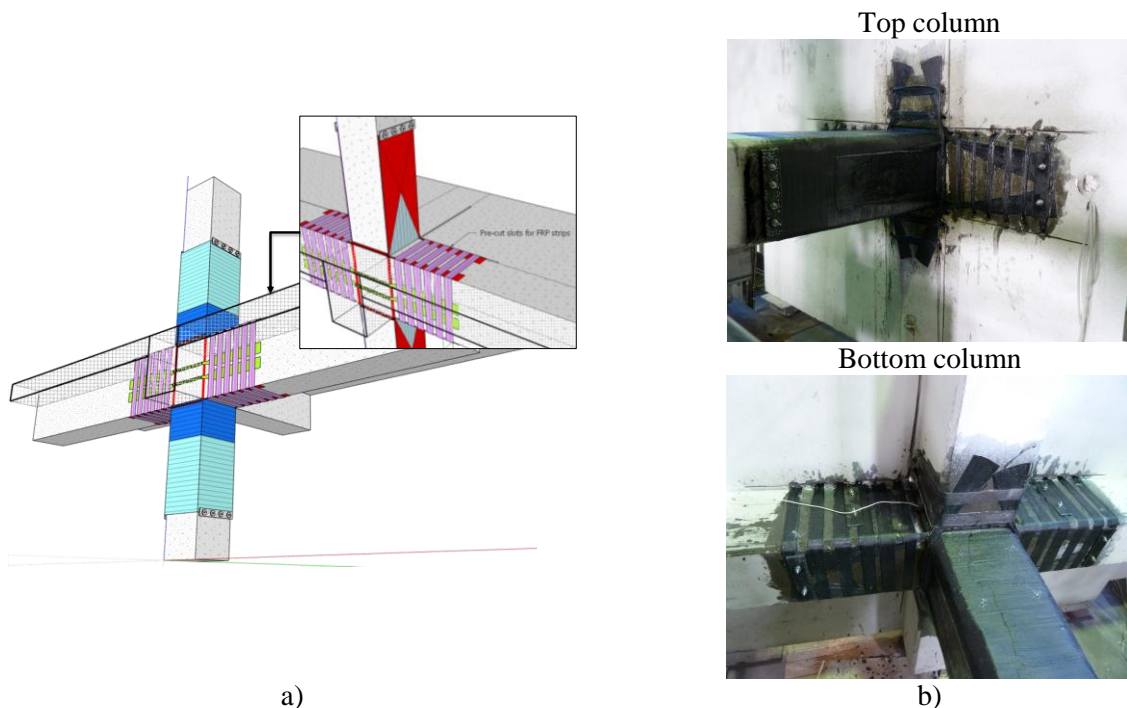


Fig. 3 – CFRP retrofit scheme: a) generic scheme; b) global view

3.2. Steel plates retrofit and repair scheme

The steel plates retrofit scheme aims to increase the strength and stiffness of the columns in order to ensure that the beam is the weak element and consequently avoid a weak-column strong-beam mechanism. Moreover, the ductility of the beam-column joint is also enhanced by providing an appropriate concrete confinement on the columns using exterior steel stirrups. Once again, the selective weakening technique used in the slab to increase rotation of the beams.

The retrofit solution is designed to increase the flexural capacity of the columns along a length equal to 750mm from the joint. Three $\phi 20$ mm steel rods per column corner are used to connect the steel devices through the slab. Four $\phi 10$ mm mechanical anchors are placed on the last two exterior steel stirrups per column face and epoxy resin is used to fill the gap between the steel profiles and the concrete. The front view of the steel devices and the moment capacity and moment demands predictions on the retrofitted specimen are shown in Fig.4. According to the moment distribution prediction, the weak element is the bottom face of the beam.

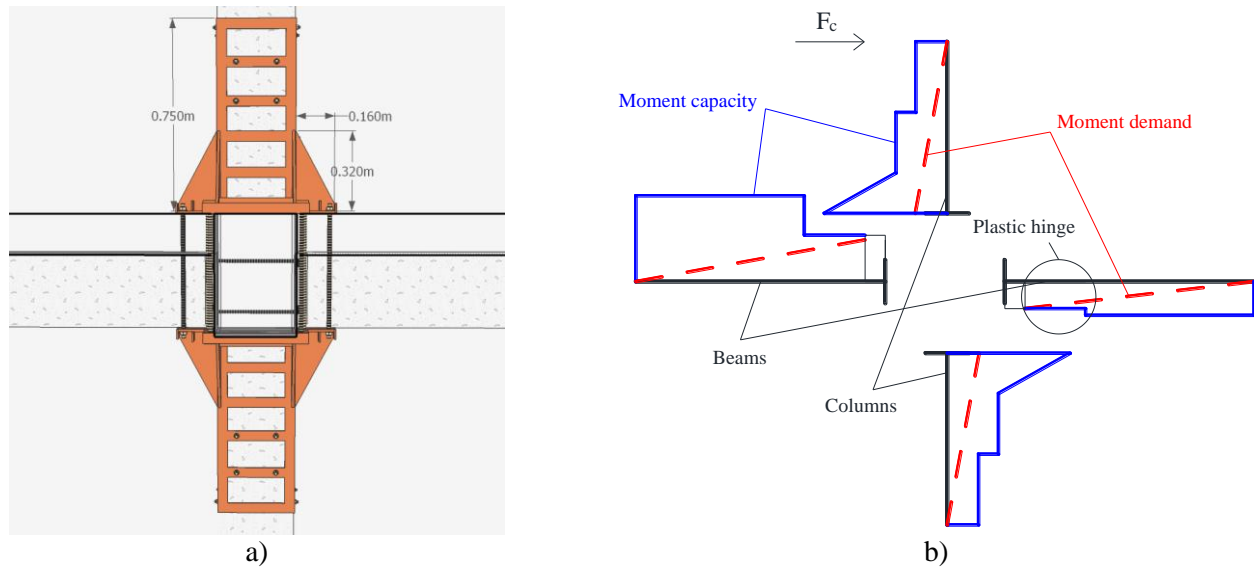


Fig. 4 – a) front view of the steel retrofit device; b) moment capacity and moment demand distribution

Each steel device is made with 40x40x3 steel L-profiles on the corners with 750mm long, six stirrups (3mm thickness and 40mm wide) and eight angles with 10mm thickness and sides with 320mm (column) and 160mm (beam). The steel components are welded in-situ to simulate real conditions. The joint core is also strengthened by two $\phi 12$ mm bars per joint face. These bars go through the beams and are anchored on 50x50x5 steel L-profiles located at the intersection of the beams. The retrofit schemes and pictures of specimen C1-RP-Steel SW are presented in Fig. 5.

The steel plates retrofit scheme requires the following steps:

1. The concrete surface under the steel plates is first roughened with a millstone;
2. The holes for the shear joint strengthening and longitudinal rods are drilled through the concrete before applying the steel plates;
3. The steel profiles and plates are placed in position and welded;
4. The mechanical anchors are applied (4 per column face);
5. The borders of the steel plates are filled with silicone to avoid epoxy resin leakage during injection;
6. Epoxy resin injection using a syringe connected to pipes placed in the corners of the column;
7. Screwing of the mechanical anchors and pre-stress of the longitudinal rods (torque = 100N.m ~ 80MPa tensile stress).

Specimen C1-RP-Steel SW is tested before specimen C1-RT-Steel SW as a trial test and as the damages are concentrated in the bottom of the beams, next to the steel devices, it is decided to strengthen the beam in that zone for specimen C1-RT-Steel SW. Therefore, the bottom face of the beam in specimen C1-RT-Steel SW is strengthened with a steel plate with dimensions 70mmx450mmx3mm and four U shaped external stirrups with a cross-section of 40mmx3mm. Mechanical anchors are also used as in Fig.6.

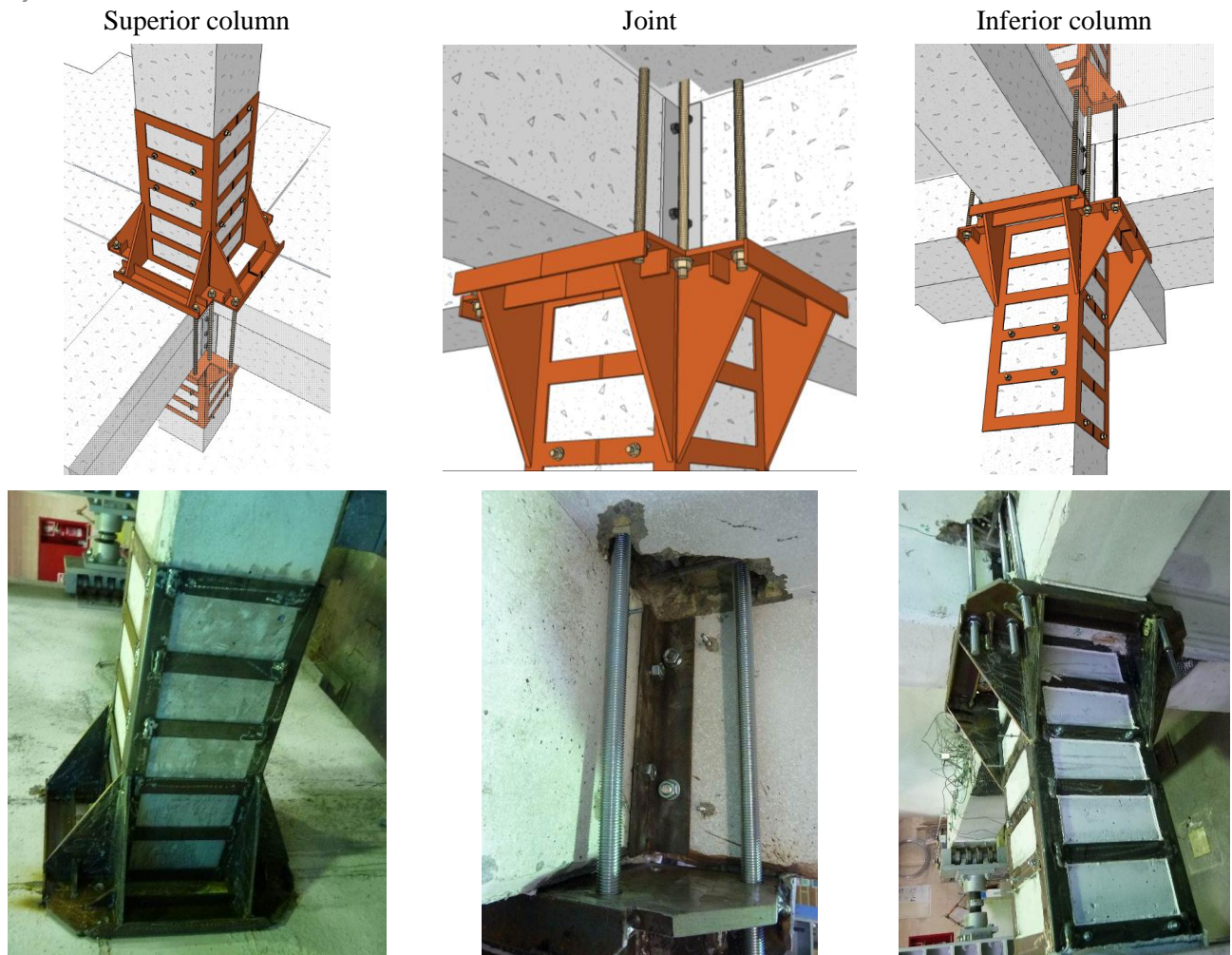


Fig. 5 – Steel retrofit schemes and pictures of specimen C1-RP-Steel SW

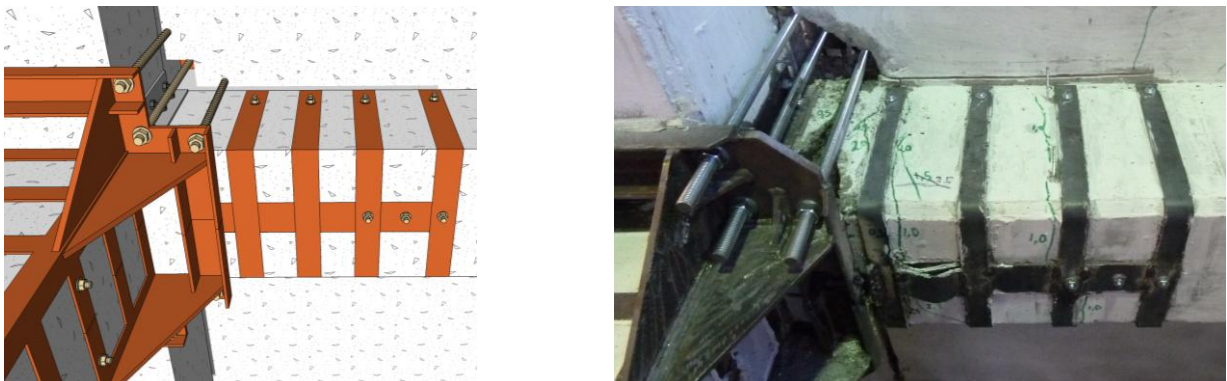


Fig. 6 – Beam strengthening of specimen C1-RT-Steel SW

For the repaired specimen C1-RP-Steel SW, the aim is to investigate whether the heavily damaged specimen C-SW could be repaired and achieve similar performance as a retrofitted specimen. The repair technique employed on specimen C-SW corresponds to a two-step approach. First the buckled bars on the superior column are cut and the damaged concrete is removed from the damaged specimen. Then, new 250 mm long bars are welded onto the non-yielded ends of the existing bars and the concrete is replaced.



4. Experimental results

In this section, the main results from the experimental campaign are presented. The hysteretic results and the evolution of the hysteretic dissipated energy with the drift level are presented. Moreover, the equivalent damping-displacement ductility relationships are provided. Several comparisons are established between the cyclic results, in terms of force-displacement relationships to show the difference in results between the retrofit solutions and between the control and the retrofitted specimens. Finally, the final damage pattern is shown and discussed. The hysteretic dissipated energy was computed for all cyclic tests performed as the sum of the area under the force-displacement diagrams. The equivalent damping (ξ_{eq}) was computed according to [10] and [11]. The displacement ductility (μ_d) corresponds to the ratio between the imposed displacement (d_c) and the yielding displacement (Δ_y). The yield displacement corresponds to the displacement when the first rebar reach the yield strain measured by the strain gauges. The ultimate force is achieved when the strength has a reduction of 20% relatively to the maximum force, as adopted by [12].

4.1. Global results

The cyclic force-displacement relationship and the corresponding envelopes obtained in the experimental tests are shown in Fig.7. Table 2 shows the values of maximum lateral force ($F_{c,max}$) and the corresponding drift ($Drift_{F_{c,max}}$), the ultimate force ($F_{c,ult}$) and corresponding drift ($Drift_{F_{c,ult}}$), and also the yielding drift of the columns ($\Delta_{y,column}$) and beams ($\Delta_{y,beam}$) measured with the strain gauges placed on the longitudinal reinforcement.

The control specimen C-SW has, as expected, a failure at a low drift value (1.6% ultimate drift) when compared to the other specimens. The failure occurs in the superior column showing the weak-column strong-beam mechanism even with cuts on the slab (selective weakening technique). The hysteretic results for the specimens retrofitted with steel plates present lower pinching effects than the specimen retrofitted with CFRP as a consequence of the elastic properties of the CFRP that does not contribute as much as the steel plates to the dissipated energy. Specimen C1-RT-B SW reaches larger drift levels due to the lower stiffness (CFRP does not change the stiffness) and the larger distribution of the damage than the specimens retrofitted with steel plates. Specimens C1-RP-Steel SW and C1-RT-Steel SW have a similar cyclic behavior but the test on the repaired specimen is stopped at 2.5% drift due to the failure in tension of the rebars located at the bottom of the right beam. The beam strengthening solution adopted for specimen C1-RT-Steel SW increases the ultimate drift by delaying buckling of the beam rebars, but the connection between the longitudinal steel plate of the beam and the steel retrofit device is lost at 1.5% drift.

The yield drifts of the columns and beams, presented in Table 2, show that the yield of the columns on the retrofitted specimens occurs for larger drift levels than in the control specimen, especially in specimen C1-RT-Steel SW. Moreover, the beam yield drifts of the retrofitted specimens tend to be smaller than in the control specimen demonstrating an early activation of the beam capacity on the retrofitted specimens and a change of failure mechanism from columns to beams.

Table 2 – Maximum and ultimate force, drift values and yield drift of columns and beams

Specimen	Max. force, $F_{c,max}$ (kN)	Drift $_{F_{c,max}}$ (%)	Ult. force, $F_{c,ult}$ (kN)	Drift $_{F_{c,ult}}$ (%)	$\Delta_{y,column}$ (%)	$\Delta_{y,beam}$ (%)
C-SW	-67.5	-1.0	54.0	1.6	0.48	0.74
C1-RT-B SW	86.9	3.5	69.5	6.0	0.95	1.20
C1-RP-Steel SW	91.2	1.5	-	-	-	0.68
C1-RT-Steel SW	-93.6	-1.0	74.9	3.9	2.47	0.48

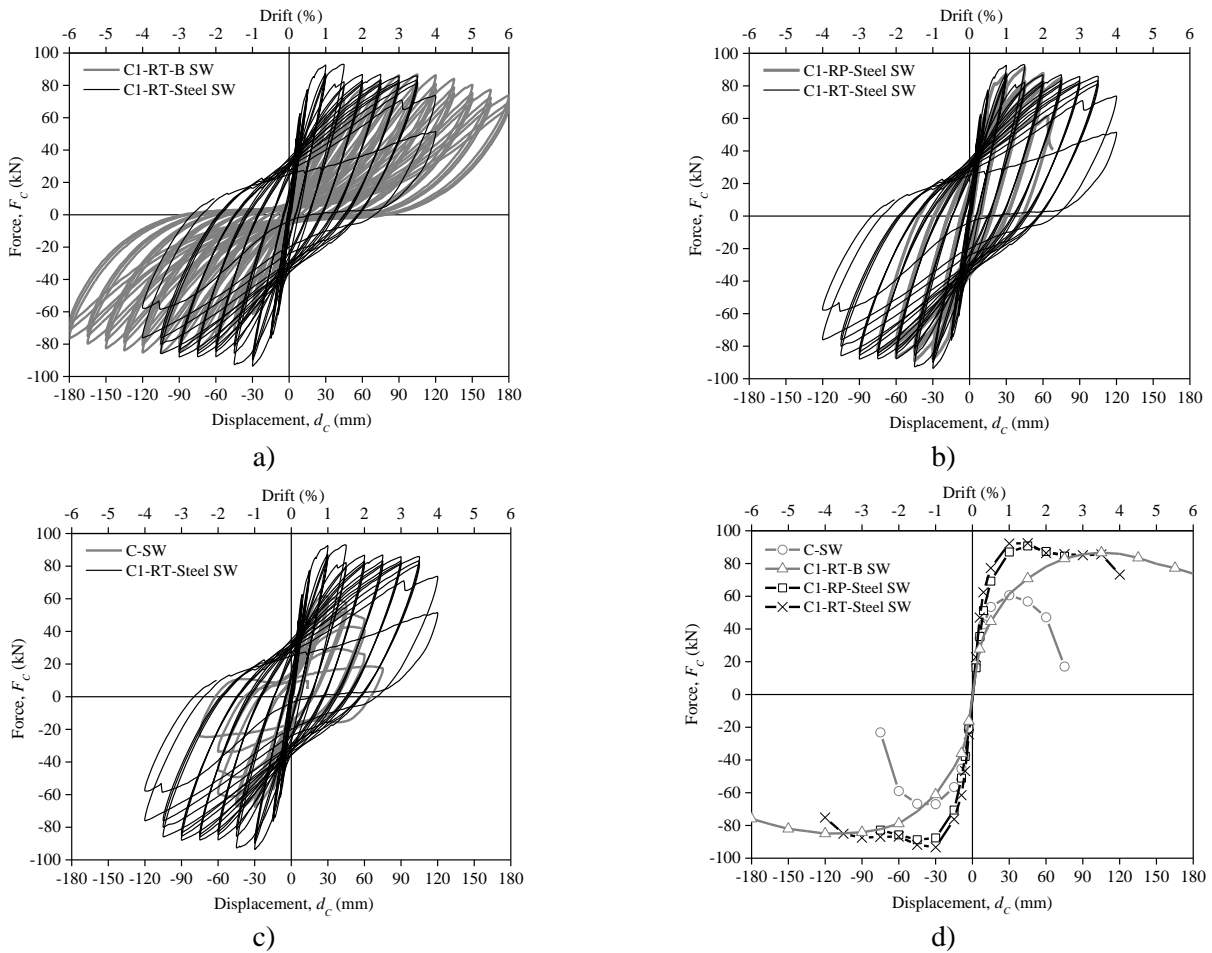


Fig. 7 – Force-displacement diagrams: a), b) and c) cyclic; d) envelopes

The dissipated energy evolution and the equivalent damping-displacement ductility results are shown in Fig. 8. Specimens retrofitted with steel plates are the ones that dissipate more energy for the each drift level as the global behavior is governed by the rebars on the beams. These reach hardening for the steel-retrofitted specimens and consequently enlarge the load-unload-reload loops. In the case of specimen C1-RT-B SW the increase in cumulative dissipated energy is not so evident due to the linear properties of the CFRP. Specimen C1-RT-Steel SW has the largest ductility despite the larger ultimate drift observed in specimen C1-RT-B SW as the yield drift in this specimen is almost twice that of specimen C1-RT-Steel SW.

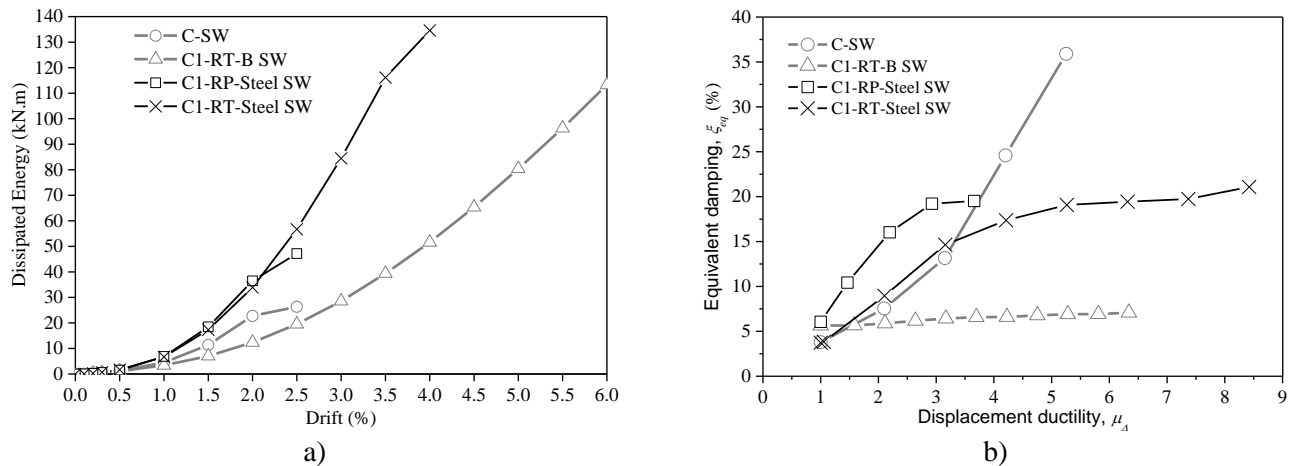


Fig. 8 – a) Dissipated energy; b) equivalent damping - ductility

4.2. Observed Damage

Fig.9 displays the damage state observed at the end of the cyclic tests. No shear damage is observed in the joint core for all specimens after test. The superior column of specimen C-SW fails in bending with concrete spalling and bar buckling and no significant damage is observed in the other elements. Damage on specimen C1-RT-B SW is distributed along the beams, slab and the column-joint interface. No significant CFRP debonding are detected during the test. A concentrated plastic hinge is observed in the beams next to the steel retrofit device in specimen C1-RP-Steel SW and concrete spalling, bar buckling and bar rupture are observed in the plastic hinge zone. In specimen C1-RT-Steel SW damage is also concentrated at the beam-joint interfaces and bar rupture at the bottom face of the beam and at the slab are seen.



C-SW



C1-RT-B SW



C1-RP-Steel SW



C1-RT-Steel SW

Fig. 9 – Damage observed at the end of the test

5. Main conclusions

Experimental tests on realistic full-scale RC beam-column joints with slab and transverse beams are performed. Repair and retrofit strategies with CFRP or steel plates for beam-column joints with typical pre-1970's deficiencies are proposed and tested. Test results are analysed in terms of maximum strength, yield drift, hysteretic dissipated energy, equivalent damping function of displacement ductility and damage state at the end of the tests.

The control specimen shows the typical seismic failure mode on non-seismically designed beam-column joints. The retrofit solution with CFRP significantly increases (+29%) the strength and ultimate drift without increasing the initial stiffness. The dissipated energy is also larger for high drift levels than in the control specimen. However, the equivalent damping of the specimen retrofitted with CFRP does not increase for large



displacement ductility demands as expected for RC elements. This is due to the linear properties of the CFRP that induce the pinching effect and the dissipated energy does not increase very much. However, the cyclic performance of specimen C1-RT-B SW is notably improved when compared to the control specimen behaviour.

The peak strength obtained on specimen C1-RT-Steel SW is also significantly larger (37%) than in the control specimen. The initial stiffness of the specimens retrofitted with steel plates is the largest due to the second moment of area increase on the columns that contributes to moving the plastic hinge from the column (control specimen) to the beams. The dissipated energy capacity and ductility is also much more significant than in the control specimen and in C1-RT-B SW.

The retrofit solutions here-presented contribute to improving the behaviour of beam-column joints and consequently the seismic performance of RC structures by increasing the strength, dissipated energy and ductility of these elements. Moreover, it is demonstrated that the cyclic behaviour of non-seismic designed elements can be significantly improved and these retrofit solutions are realistic and easy to install in a real RC structure.

6. Acknowledgements

This research is funded as part of the Challenging RISK project funded by EPSRC (EP/K022377/1). The authors acknowledge the staff of the Civil Laboratory at the University of Aveiro for the support during the experimental campaign. The CFRP material used in this experimental campaign was kindly provided by S&P reinforcement.

7. References

- [1] Rosseto T, Peiris N, Alarcon J, So E, Sargeant S, Sword-Daniels V, Libberton C, Verrucci E, Re D, Free M. (2009): The L'Aquila, Italy Earthquake of 6 April 2009 – a preliminary field report by EEFIT. The Earthquake Engineering Field Investigation Team, University College London.
- [2] Ricci P, De Luca F, Verderame GM (2011): 6th April 2009 L'Aquila earthquake, Italy: reinforced concrete building performance. *Bulletin of Earthquake Engineering*, **9**(1), 285–305.
- [3] Pohoryles D, Melo J, Rosseto T, Varum H, D'Ayala D (2015): Experimental Investigation on the Seismic FRP Retrofit of Realistic Full-Scale RC Beam-Column Joints. *Second ATC & SEI Conference on Improving the Seismic Performance of Existing Buildings and Other Structures*, San Francisco.
- [4] Akguzel U, Pampanin S (2010): Effects of Variation of Axial Load and Bidirectional Loading on Seismic Performance of GFRP Retrofitted Reinforced Concrete Exterior Beam-Column Joints. *Journal of Composites for Construction*, **14**(1), 94–104. DOI: 10.1061/(ASCE)1090-0268(2010)14:1(94).
- [5] Pohoryles D, Rosseto T, Melo J, Varum H (2016): A combined FRP and selective weakening retrofit for realistic pre-1970's RC structures, ICONHIC 2016 - 1st International Conference on Natural Hazards & Infrastructure. Chania, Greece.
- [6] Governo D. (1967): Regulamento de Estruturas de Betão Armado (REBA), Decreto n.º 47723, 20 de Maio, serie I, num. 119, Lisbon. (in Portuguese)
- [7] CEN, NP EN 1992-1-1 (2010): Eurocode 2, Design of concrete structures. Part 1-1: General rules and rules for buildings. European Committee for Standardization, Brussels, Belgium.
- [8] Pampanin S, Akguzel U (2011): Performance-Based Seismic Retrofit of Existing Reinforced Concrete Frame Buildings using Fibre-Reinforced Polymers: Challenges and Solutions. *Structural Engineering International*, **21**(3), 260–270. DOI: 10.2749/101686611X13049248220041.
- [9] Pohoryles D, Melo J, Rosseto T, Varum H, D'Ayala D (2017): A realistic full CFRP retrofit of RC beam-column joints compared to seismically designed specimens, 16th World Conference on Earthquake Engineering, 16WCEE 2017, Santiago, Chile.
- [10] Varum, H. (2003): *Seismic assessment, strengthening and repair of existing buildings*, PhD Thesis, University of Aveiro, Portugal.
- [11] Priestley M, Calvi G, Kowalsky M (2007): *Displacement-Based Seismic Design of Structures*, IUSS PRESS, Italy.



- [12] Park Y J, Ang A H S, Wen Y K, (1987): Damage-limiting aseismic design of buildings, *Earthquake Spectra*, **3** (1), 1-26.